Cell Transplantation, Vol. 26, pp. 983–1000, 2017
Printed in the USA.

0963-6897/17 $90.00 + .00
DOI: https://doi.org/10.3727/096368917X694697
E-ISSN 1555-3892
www.cognizantcommunication.com

Early Subretinal Allograft Rejection Is Characterized by Innate Immune Activity

Kevin P. Kennelly,*† Toby M. Holmes,‡ Deborah M. Wallace,*
Cliona O'Farrelly,§¶ and David J. Keegan*†

*School of Medicine, University College Dublin, Dublin, Ireland
†Department of Ophthalmology, Mater Misericordiae University Hospital, Dublin, Ireland
‡School of Clinical Dentistry, University of Sheffield, Sheffield, UK
§School of Biochemistry and Immunology, Trinity College Dublin, Dublin, Ireland
¶School of Medicine, Trinity College Dublin, Dublin, Ireland

Successful subretinal transplantation is limited by considerable early graft loss despite pharmacological suppression of adaptive immunity. We postulated that early innate immune activity is a dominant factor in determining graft survival and chose a nonimmunosuppressed mouse model of retinal pigment epithelial (RPE) cell transplantation to explore this. Expression of almost all measured cytokines by DH01 RPE cells increased significantly following graft preparation, and the neutrophil chemoattractant KC/GRO/CINC was most significantly increased. Subretinal allografts of DH01 cells (C57BL/10 origin) into healthy, nonimmunosuppressed C57BL/6 murine eyes were harvested and fixed at 1, 3, 7, and 28 days postoperatively and subsequently cryosectioned and stained. Graft cells were detected using SV40 large T antigen (SV40T) immunolabeling and apoptosis/necrosis by terminal deoxynucleotidyl transferase dUTP nick-end labeling (TUNEL). Sections were also immunolabeled for macrophage (CD11b and F4/80), neutrophil (Gr1 Ly-6G), and T-lymphocyte (CD3-ε) infiltration. Images captured with an Olympus FV1000 confocal microscope were analyzed using the Imaris software. The proportion of the subretinal bolus comprising graft cells ($SV40T^+$) was significantly ($p<0.001$) reduced between postoperative day (POD) 3 (90±4%) and POD 7 (20±7%). $CD11b^+$, $F4/80^+$, and Gr1 $Ly\text{-}6G^+$ cells increased significantly ($p<0.05$) from POD 1 and predominated over $SV40T^+$ cells by POD 7. Colabeling confocal microscopic analysis demonstrated graft engulfment by neutrophils and macrophages at POD 7, and reconstruction of z-stacked confocal images confirmed SV40T inside Gr1 $Ly\text{-}6G^+$ cells. Expression of CD3-ε was low and did not differ significantly between time points. By POD 28, no graft cells were detectable and few inflammatory cells remained. These studies reveal, for the first time, a critical role for innate immune mechanisms early in subretinal graft rejection. The future success of subretinal transplantation will require more emphasis on techniques to limit innate immune-mediated graft loss, rather than focusing exclusively on suppression of the adaptive immune response.

Key words: Retinal transplantation; Innate immunity; Cell transplantation; Retinal pigment epithelium (RPE); Neutrophil; Macrophage

INTRODUCTION

Retinal degenerative diseases, including neovascular and nonneovascular age-related macular degeneration, are the most common causes of blindness in the developed world[1]. Anti-vascular endothelial growth factor (anti-VEGF) agents prevent loss of vision and improve visual acuity in patients with neovascular degeneration[2–4]. However, no effective treatment exists for nonneovascular degeneration, which is more common[5]. Transplantation of cells into the subretinal space (SRS) to replace degenerating or dysfunctional cells has been proposed as a treatment strategy[6] and rescues anatomical features and vision in animal models of retinal degenerative disease[7–22] as well as affected human patients[23–25].

Rapid loss of grafted cells and decreases in anatomical and functional benefits following transplantation[26,27] remain major challenges. This occurs despite suppression of the T-lymphocyte-mediated adaptive immune response with drugs such as cyclosporine and azathioprine. These immunosuppressive regimes still have graft survival rates of just 11% at 4 weeks[28,29] and 0.2% at 28 weeks[28]. Indeed, rabbit allograft failure is not associated with lymphocyte

Received Febraury 19, 2015; final acceptance January 20, 2017. Online prepub date: January 20, 2017.
Address correspondence to David Keegan, Department of Ophthalmology, Mater Misericordiae University Hospital, Eccles Street, Dublin 7, Ireland. Tel: +35318307059; Fax: +35318307198; E-mail: dkeegan@mater.ie

infiltration and is not altered by cyclosporine immunosuppression[30,31].

Poor graft survival in the SRS is paradoxical, as this site is characterized by a suppressed antigen-specific adaptive immune response[32–34]. Retinal pigment epithelial (RPE) cells express the CD95 ligand that induces T-cell apoptosis, secrete transforming growth factor-β (TGF-β), which is important in the induction of tolerance[35], and can also phagocytose T lymphocytes[36]. We hypothesized that cells transplanted into the immune-deviant SRS are destroyed by an alternate immune mechanism rather than via the classic T-lymphocyte-mediated immunological rejection.

Innate immune responses are characterized by upregulation of proinflammatory cytokines[37] and a coordinated local and systemic inflammatory response[38]. A critical role for innate immunity in acute allograft rejection is now emerging[39–41] and has been shown to be crucial in skin[42] and pancreatic islet[43] allograft rejection. However, the role of innate immunity in subretinal transplantation has not been studied. We hypothesized that subretinal graft failure is a consequence of innate immune mechanisms and used a mouse RPE allograft model to investigate this. The purpose of this study was to examine the mechanisms underlying early allograft cell loss in the SRS rather than to achieve a structural or functional benefit following transplantation. Accordingly, we used healthy nonimmunosuppressed hosts to investigate our hypothesis.

MATERIALS AND METHODS

Ethics Statement

Ethical approval for this research was obtained from Animal Research Ethics Committee (AREC-P-07-09-Keegan). All procedures involving the use of mice were performed in accordance with the Association for Research in Vision and Ophthalmology (ARVO) Statement for the Use and Care of Animals in Ophthalmic and Vision Research, and all efforts were made to minimize suffering.

Cell Line Derivation

The DH01 RPE line was prepared from RPE cultured from a healthy C57BL/10.RIII-H-2r mouse as previously described[44] and immortalized using supernatant from the SVU 19.5 cell line[45] secreting retrovirus encoding a temperature-sensitive non-SV40 origin-binding U19 mutant of the SV40T antigen and the neomycin resistance gene[46].

Cell Culture

DH01 cells were routinely cultured in high-glucose Dulbecco's modified Eagle's medium (DMEM) (Sigma-Aldrich Ireland, Wicklow, Ireland) supplemented with 1% fetal calf serum (FCS; Sigma-Aldrich Ireland), 200 mM L-glutamine (Sigma-Aldrich Ireland), and 5 mg/ml penicillin/streptomycin (Sigma-Aldrich Ireland). As these cells harbor SV40T, they were grown at 33°C in 5% CO_2.

Transplant Conditions (TC) and Baseline Conditions (BC)

TC cells were prepared as a highly concentrated cell suspension (50,000 cells/μl), deprived of serum (suspended in serum-free medium), and kept on ice for the maximum period that typically exists between harvesting and transplanting the graft (4 h). To determine the effect of graft cell suspension preparation on cytokine production, we compared cytokine expression by DH01 cells immediately following resuspension in full media (BC) and after being prepared for subretinal transplantation (TC).

Preparation of Samples for Cytokine Quantification

Cytokine production by DH01 was quantified under BC and following the stress of the graft cell suspension preparation procedure (TC). Cells were cultured in full medium, trypsinized (Sigma-Aldrich Ireland), and seeded in triplicate in 24-well culture plates with 2×10^5 cells/well to yield confluent cultures. BC cells were seeded in 0.5 ml of serum-free medium. TC cells were subjected to the process involved in the preparation of a graft cell suspension as described above and, after 4 h on ice, were seeded in 0.5 ml of serum-free medium. Following culture for 24 h, the medium was removed and stored at −80°C for subsequent analysis.

Multiplex Cytokine Assay

A nine-plex multispot T helper 1 (TH1)/TH2 cytokine assay kit [K15013B-1; Meso Scale Discovery (MSD), Rockville, MD, USA] was used according to the manufacturer's instructions to quantify the following cytokines: interferon-γ (IFN-γ), tumor necrosis factor-α (TNF-α), interleukin-1β (IL-1β), IL-2, IL-4, IL-5, IL-10, IL-12, and keratinocyte chemoattractant/growth regulated oncogene-α/cytokine-induced neutrophil chemoattractant (KC/GRO/CINC). An 8-point calibration curve from 0 to 10,000 pg/ml was constructed using a plot of signal intensity from a series of known concentrations of the multiplex standard provided by the kit manufacturer. Cytokine levels were calculated using the MSD Sector Imager 2400 and Discovery Software 2.0 (MSD). Concentrations were determined in triplicate and expressed in pg/ml.

IL-6 Enzyme-Linked Immunosorbent Assay (ELISA)

IL-6 was not included on the MSD TH1/TH2 multiplex kit. Therefore, expression of this cytokine was measured separately using an IL-6 ELISA kit (KMC0061; Invitrogen, Carlsbad, CA, USA). A 6-point calibration curve from 0 to 500 pg/ml was generated from standard mouse IL-6 reconstituted in standard diluent buffer. ELISA was carried

out as per the manufacturer's instructions. Absorbance at 450 nm was measured using a spectrophotometer (SpectraMax M2; Molecular Devices, Sunnyvale, CA, USA). Sample IL-6 concentrations were calculated against the graph of the standard curve. Concentrations were determined in triplicate and expressed in pg/ml.

Subretinal RPE Cell Transplantation

Male C57BL/6 mice were obtained from Harlan (Bicester, UK). All surgery was performed under ketamine (Ketalar; 75 mg/kg; C&M Vetlink, Limerick, Ireland) and medetomidine (Domitor; 0.5 mg/kg; C&M Vetlink) anesthesia, and the mice were recovered with atipamezole (Antisedan; 1 mg/kg; C&M Vetlink). Euthanasia was with sodium pentobarbitone (Euthatal; 140 mg/kg; C&M Vetlink) followed by cervical dislocation. All drugs were delivered by intraperitoneal (IP) injection, with the exception of atipamezole, which was delivered by subcutaneous injection.

DH01 (C57BL/10 origin) cell suspensions (50,000 cells/μl DMEM) were prepared from preconfluent cultures as described under TC above. We have previously demonstrated that preparing DH01 cell suspensions in this manner results in 95% graft cell viability at the time of transplantation[44]. Subretinal transplants were delivered transsclerally through glass microinjection pipettes (BioMedical Instruments, Zollnitz, Germany) to the dorsotemporal SRS of healthy nonimmunosuppressed C57BL/6 mice. Eyes received 2 μl of the graft cell suspension ($n=16$). Graft position and size were verified by fundoscopy under the operating microscope. To distinguish a host inflammatory response to the surgical procedure, as distinct from a response directed specifically against the allograft, sham surgery with controls that received 2 μl of vehicle only (serum-free medium) was also performed ($n=16$). The animals were euthanized, and the eyes were harvested on postoperative day (POD) 1, 3, 7, and 28 ($n=4$/group/time point). In order to establish the baseline expression of markers of interest, unoperated eyes were also harvested from naive mice that received neither graft nor sham surgery to either eye ($n=4$). The eyes were fixed in 4% paraformaldehyde (PFA), cryoprotected in sucrose, embedded in optimal cutting temperature (OCT) compound (Tissue-Tek; Sakura Finetek, Dublin, Ireland) under liquid nitrogen, and stored at −80°C. Sections (7 μm) were cut on a Leica (Wetzlar, Germany) CM1900 UV cryostat and stained as described below.

Graft Detection (SV40T), TUNEL Labeling, and Identification of the Host Immune Response to Subretinal RPE Transplants

To examine temporal graft survival, graft cells were identified using a specific primary antibody to SV40T (SC-20800; 1:100; Santa Cruz Biotechnology, Dallas, TX, USA) and goat anti-rabbit Texas Red-labeled secondary antibody (111-075-003; 1:100; Jackson Immuno Research Laboratories, West Grove, PA, USA). DNA strand breaks were detected by terminal deoxynucleotidyl transferase dUTP nick end labeling (TUNEL) as previously described[47].

To examine the host immune response to subretinal DH01 allografts, cryosections were immunolabeled for the SV40T antigen (SC-20800; 1:100; Santa Cruz Biotechnology) using a donkey anti-rabbit fluorescein isothiocyanate (FITC)-labeled secondary antibody (711-095-152; 1:100; Jackson ImmunoResearch Laboratories). In addition, sections were immunolabeled to detect macrophages (CD11b and F4/80), neutrophils (Gr1 Ly-6G), or T lymphocytes (CD3-ε). Rat anti-mouse CD11b (MCA711; 1:100; AbD Serotec, Oxford, UK), rat anti-mouse F4/80 (MCA 497EL; 1:25; AbD Serotec), and rat anti-mouse Gr1 Ly-6G (MAB1037; 1:100; R&D Systems, Minneapolis, MN, USA) primary antibodies were secondarily immunolabeled using donkey anti-rat tetramethylrhodamine (TRITC)-labeled secondary antibody (712-025-150; 1:50; Jackson ImmunoResearch Laboratories). Goat anti-mouse CD3-ε (sc-1127; 1:100; Santa Cruz Biotechnology) was secondarily immunolabeled using donkey anti-goat TRITC-labeled secondary antibody (705-025-003; 1:100; Jackson ImmunoResearch Laboratories).

Nonspecific secondary antibody binding was blocked using serum (1:50) from the host species of the secondary antibody. 4,6-Diamidino-2-phenylindole (DAPI; 10 ng/ml; D9542; Sigma-Aldrich Ireland) counterstaining was used to enable visualization of nuclei. Phosphate-buffered saline (PBS; Sigma-Aldrich Ireland) was used to dilute all reagents and for three 5-min washes between steps. After the final wash, sections were mounted using Vectashield® HardSet™ (Vector Laboratories, Peterborough, UK).

Confocal Microscopy

Immunolabeling was visualized using an Olympus (Tokyo, Japan) FluoView™ FV1000 confocal laser scanning microscope. Differential interference contrast microscopy (DIC) images were taken at the time of fluorescence confocal microscopy to more accurately identify the SRS. Z-stack images were taken through areas of interest to enable three-dimensional (3D) image reconstruction using an image analysis software as described below. Captured images were viewed using Olympus Fluoview Ver. 1.4a software.

Image Analysis

Four transplanted eyes and four sham-treated eyes were examined for each postoperative time point. Four unoperated eyes were also examined. In order to maintain consistency in analyses of transplanted eyes,

cryosections through the center of the subretinal cell bolus where the greatest numbers of cells were present were used for all eyes. For sham-treated eyes, cryosections in the region of the injection site were used. All sections were immunolabeled for SV40T to identify transplanted cells and counterstained with DAPI to label all nuclei. Sections were also immunolabeled to detect one of the following: DNA nicks (TUNEL), macrophages (CD11b and F4/80), neutrophils (Gr1 Ly-6G), or T cells (CD3-ε).

Single optical sections from four transplanted eyes and four sham-treated eyes per time point, in addition to four unoperated control eyes, were analyzed using the Imaris image analysis software (Bitplane AG, Zurich, Switzerland). For sections fluorescently labeled to detect both SV40T and TUNEL, the following counts of cells in the SRS were performed: total number of cells ($DAPI^+$), number of graft cells ($DAPI^+/SV40T^+$), and number of graft cells with DNA nicks ($DAPI^+/SV40T^+/TUNEL^+$). As the total number of cells in the SRS varied between images, the proportion of the subretinal cell bolus comprising grafted cells was calculated as $SV40T^+$ cells per 100 cells ($DAPI^+$) in the SRS. The proportion of graft cells ($SV40T^+$) that had DNA nicks ($SV40T^+/TUNEL^+$) was also calculated.

As immune cell infiltration of the SRS was identified by cell-specific surface markers (CD11b, F4/80, Gr1 Ly-6G, and CD3-ε), it was not possible to accurately estimate cell number. Therefore, sections immunolabeled for these markers in conjunction with the graft cell marker (SV40T) were analyzed by calculating the area of immunolabeling using Imaris. To correct for differing sizes of subretinal boluses, the numbers of nuclei (DAPI) in the SRS were also counted, and the areas of immunolabeling were expressed as $\mu m^2/100$ nuclei in the SRS. This enabled determination of the temporal change in expression of the graft cell marker (SV40T) relative to markers of infiltrating immune cells.

The proportion of the area of $SV40T^+$ immunolabeling that colabeled with immune cell markers (CD11b, F4/80, Gr1 Ly-6G, and CD3-ε) was also calculated using Imaris. This allowed determination of altered temporal colabeling of the graft cell marker with markers of infiltrating cells.

Z-stack confocal images of selected regions of SV40T colabeling with immune cell markers were processed using Imaris and reconstructed in 3D form using isosurface rendering to determine the nature of the relationship between colabeling markers at a cellular level.

Statistical Analysis

Data were analyzed using GraphPad Prism 5 statistical software (GraphPad, San Diego, CA, USA). Data are expressed as mean ± standard deviation (SD), and a value of $p < 0.05$ was considered statistically significant.

Comparisons of Cytokine Levels. Student's *t*-tests assuming unequal variances were used to determine the significance of differences between sample means. Results are presented as mean ± SD.

Comparisons of Cell Numbers in the SRS at Different Postoperative Time Points. At POD 1, 3, 7, and 28, counts of cells in the SRS were performed to determine the total number of cells, the proportion of cells expressing SV40T, and the proportion of $SV40T^+$ cells that were also $TUNEL^+$. One-way analysis of variance (ANOVA) followed by all pairwise post hoc *t*-tests with Bonferroni correction were used to determine the significance of differences between sample means.

Analysis of Areas of Immunolabeling. The areas of immunolabeling and the total numbers of nuclei in the SRS were calculated for each immunolabeling combination at POD 1, 3, 7, and 28. Thus, areas of immunolabeling/100 nuclei were determined. To assess changes in marker expression between time points, areas of immunolabeling/100 nuclei were treated as normally distributed and analyzed with ANOVA and Tukey's post hoc test.

Analysis of Immunofluorescence Colabeling. The proportions of SV40T immunolabeling that colabeled with immunolabeled infiltrating cells were calculated using Imaris. The colabeling proportions are likely not normally distributed and were analyzed with nonparametric methods, Kruskal–Wallis test, and Dunn's post hoc comparisons.

RESULTS

Cytokine Expression Increases Significantly Following Graft Preparation

Cytokine expression by the mouse RPE cell line DH01 was quantified under BC and TC prior to transplantation (Table 1). With the exception of IL-4, expression of all cytokines increased significantly ($p < 0.05$) following graft preparation (TC). However, KC/GRO/CINC was expressed at considerably greater levels under both BC and TC, compared to all other cytokines measured. KC/GRO/CINC also had the greatest increase (sixfold increase; $p = 0.022$) in expression following TC. A threefold increase (all $p \leq 0.001$) in expressed IL-1β, IL-5, IL-6, and IL-12 occurred following TC. There was also significantly increased expression of IL-10 (2.1-fold increase; $p = 0.024$) and IL-2 (2.7-fold increase; $p = 0.002$) following graft preparation (TC) compared to baseline levels (BC).

Table 1. DH01 Cytokine Expression Under BC and TC

Cytokine	BC*	TC*	Fold Increase	*p*
IFN-γ	1.8±0.2	2.8±0.2	1.6	0.003
IL-10	33.9±4.6	70.8±12.4	2.1	0.024
IL-12	3.4±0.9	10.2±0.9	3	<0.001
IL-1β	1±0.2	3±0.3	3.1	<0.001
IL-2	11.3±1.6	30±2.9	2.7	0.002
IL-4	6.2±0.5	8.2±1.4	1.3	0.128
IL-5	1.7±0.5	5.2±0.4	3.1	0.001
KC/GRO/CINC	591.8±15.1	3,580.9±790.2	6.1	0.022
TNF-α	0±0	5.1±0.7	N/A	0.007
IL-6	44.9±3.5	137.2±3.7	3.1	<0.001

*Values represent pg/ml and are expressed as mean±standard deviation (SD).

Retinas From Unoperated and Sham-Treated Eyes of C57BL/6 Mice Contain F4/80⁺ Cells and Few TUNEL⁺ Cells, But Do Not Contain CD11b⁺, Gr1 Ly-6G⁺, or CD3-ε⁺ Cells

To establish the baseline expression of markers of interest in the C57BL/6 mouse retina, cryosections from unoperated eyes ($n=4$) and sham-treated eyes at POD 1, 3, 7, and 28 ($n=4$/time point) were labeled for macrophage (CD11b and F4/80), neutrophil (Gr1 Ly-6G), and T-lymphocyte (CD3-ε) markers. TUNEL labeling was also performed to examine baseline apoptosis and necrosis in the retina. All sections were additionally labeled for SV40T to establish levels of background staining for the graft cell marker. All nuclei were counterstained with DAPI (Fig. 1).

The unoperated retina was characterized by the presence of F4/80⁺ cells, particularly in the ganglion cell layer (Fig. 1k). Low background levels of TUNEL⁺ cells were also present in the retina (Fig. 1a). SV40T, CD11b, Gr1 Ly-6G, or CD3-ε labeling was not observed, and no cells were present in the SRS.

Sham-treated eyes did not demonstrate SV40T immunolabeling but had low levels of TUNEL⁺ cells in the inner and outer nuclear layers of the retina (Fig. 1b–e). At all postoperative time points, sham-operated eyes did not have cells in the SRS, and the retina did not stain for CD11b, Gr1 Ly-6G, or CD3-ε. However, F4/80⁺ cells were seen in retinas of sham-operated eyes, particularly in the ganglion cell layer in a pattern analogous to that observed in unoperated eyes (Fig. 1l–o).

The First Week Posttransplantation Is Characterized by Rapid Loss of DH01 RPE Allograft Cells But Low Levels of Graft Apoptosis and Necrosis

We sought to ascertain whether apoptosis or necrosis was a predominant mechanism of graft failure in the early postoperative period. DH01 (C57BL/10 origin) cell suspension allografts (in serum-free medium) were transplanted into the SRS of C57BL/6 mice. Subretinal DH01 allografts were examined at POD 1, 3, 7, and 28 ($n=4$ eyes/time point). Cryosections were immunohistochemically labeled for SV40T (Texas Red) to identify transplanted cells and TUNEL labeled (FITC, green) to examine for DNA strand nicks. All nuclei were identified using DAPI (blue) counterstaining.

Subretinal DH01 allograft cells were distinguishable from host cells by SV40T immunolabeling (Fig. 2A). At POD 1 and POD 3, most cells in the subretinal bolus were identified as graft cells by the expression of the SV40T in the nucleus (Fig. 2Aa and b). By POD 7, there was a dramatic reduction in the proportion of cells in the subretinal bolus expressing SV40T (Fig. 2Ac). TUNEL labeling demonstrated that few cells in the subretinal bolus had DNA strand nicks at each time point. No graft cells were identified at POD 28 (Fig. 2Ad). Few cells in the nuclear layers of the retina were TUNEL⁺ following subretinal cell transplantation (Fig. 2Aa–d). This observation relates to the retinal detachment induced to place the graft and was also evident in sham-treated eyes (Fig. 1b–e).

Cell counts were performed using Imaris image analysis software. The proportion of all cells (DAPI⁺) identifiable as graft cells (DAPI⁺/SV40T⁺) in the SRS was quantified. The proportion of graft cells (DAPI⁺/SV40T⁺) with DNA strand nicks (DAPI⁺/SV40T⁺/TUNEL⁺) was also quantified. There was no significant change in the total number of cells in the SRS between POD 1 (435±143), POD 3 (487±164), and POD 7 (607±45), but total cell number decreased significantly ($p<0.05$) between POD 7 (607±45) and POD 28 (49±49) (Fig. 2B). There was no significant difference in the proportion of the subretinal bolus composed of graft cells between POD 1 (93±1%) and POD 3 (90±4%) (Fig. 2C). However, there was a significant ($p<0.001$) reduction in the proportion of the subretinal bolus composed of graft cells between POD 3 (90±4%) and POD 7 (20±7%) (Fig. 2C). No graft cells survived to POD 28. Levels of graft cells with DNA

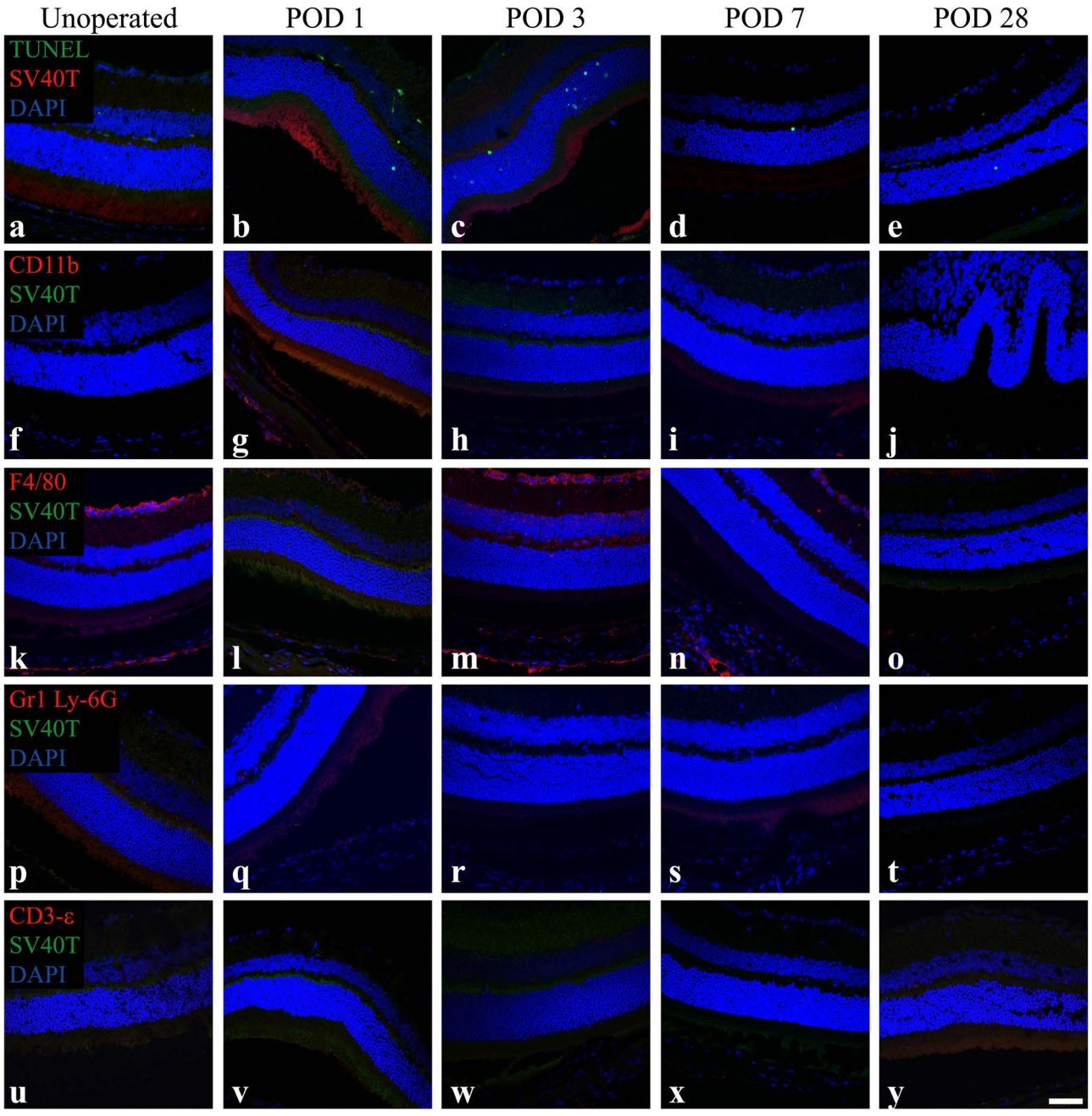

Figure 1. Retinas from unoperated and sham-treated eyes of C57BL/6 mice contain F4/80$^+$ cells and few terminal deoxynucleotidyl transferase dUTP nick-end labeling-positive (TUNEL$^+$) cells, but do not contain SV40T$^+$, CD11b$^+$, Gr1 Ly-6G$^+$, or CD3-ε$^+$ cells. Representative confocal microscopy images of sections from unoperated and sham-treated eyes immunolabeled for SV40 large T antigen (SV40T) (Texas Red: a–e; fluorescein isothiocyanate (FITC), green: f–y) to identify background expression of the graft cell marker and either TUNEL (FITC, green) to identify DNA strand nicks in apoptotic and necrotic cells (a–e) or immunolabeled for the immune cell surface markers CD11b (f–j), F4/80 (k–o), Gr1 Ly-6G (p–t), or CD3-ε (u–y) [all tetramethylrhodamine (TRITC), red]. All nuclei were counterstained with 4,6-diamidino-2-phenylindole (DAPI, blue). Unoperated and sham-treated retinas had F4/80$^+$ cells in the inner retina. Low background levels of TUNEL$^+$ cells were evident in the inner and outer nuclear layers, particularly on postoperative days (POD) 1 and 3. SV40T$^+$, CD11b$^+$, Gr1 Ly-6G$^+$, or CD3-ε$^+$ cells were not observed. Scale bar: 50 μm.

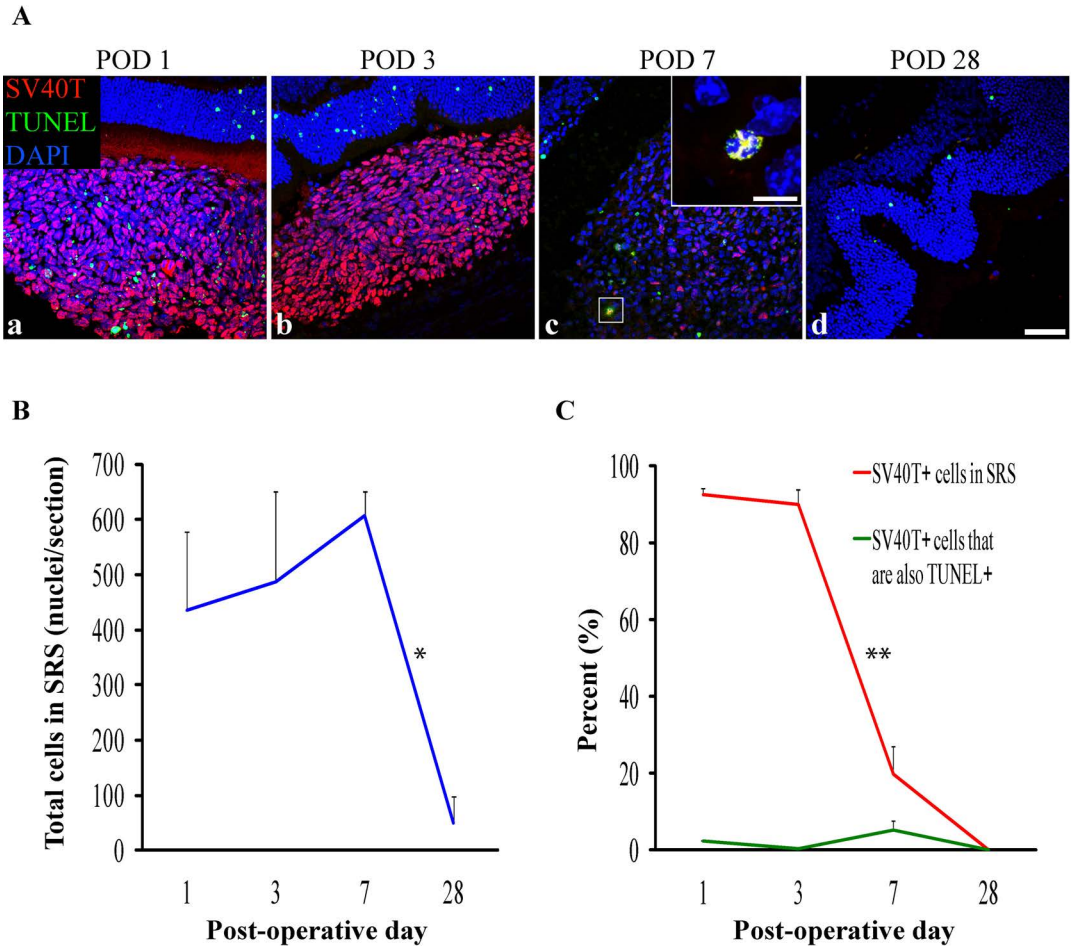

Figure 2. DH01 retinal pigment epithelial (RPE) cells allografted to the subretinal space (SRS) of healthy nonimmunosuppressed C57BL/6 mice are lost by POD 28. (A) Representative confocal microscopy images of sections immunolabeled for SV40T (Texas Red) to identify transplanted cells and TUNEL (FITC, green) to identify DNA strand nicks in apoptotic and necrotic cells. All nuclei were counterstained with DAPI (blue). At POD 1 (a) and POD 3 (b) most cells in the subretinal bolus are graft cells ($SV40T^+$). However, few transplanted cells are seen at POD 7 (c), and no graft cells remain at POD 28 (d). TUNEL labeling in the subretinal cell bolus remains low at each time point. High-power inset at POD 7 (c) shows an example of an apoptotic/necrotic graft cell ($DAPI^+$/$SV40T^+$/$TUNEL^+$). Scale bars: 50 μm, 10 μm [high-power inset in (c)]. (B) There was no significant change in the total number of cells in the SRS between POD 1 (435±143), POD 3 (487±164), and POD 7 (607±45), but the total cell number decreased significantly (*$p<0.05$) between POD 7 (607±45) and POD 28 (49±49). (C) The proportion of the subretinal bolus (red line) composed of graft cells did not change significantly between POD 1 (93±1%) and POD 3 (90±4%). However, there was a significant (**$p<0.001$) reduction in the proportion of the subretinal bolus composed of graft cells between POD 3 (90±4%) and POD 7 (20±7%). No graft cells survived to POD 28. Levels of graft cell apoptosis/necrosis ($DAPI^+$/$SV40T^+$/$TUNEL^+$) (green line) were low at each time point (POD 1: 2±0.3%; POD 3: 0.4±0.3%; POD 7: 5±2%) and did not differ significantly between time points.

strand nicks remained low at every time point (POD 1: 2±0.3%; POD 3: 0.4±0.3%; and POD 7: 5±2%) and did not differ significantly between time points (Fig. 2C).

The Period of Graft Loss Is Characterized by Infiltrating Cells Expressing Markers of Innate Immunity, But Not T lymphocytes

Figure 2 illustrates a significant ($p<0.001$) decrease in the proportion of cells in the subretinal bolus expressing SV40T between POD 3 and POD 7, with total graft cell loss by POD 28. Subretinal DH01 allografts were also examined at POD 1, 3, 7, and 28 ($n=4$ eyes per time point) for evidence of infiltrating macrophages ($CD11b^+$ and $F4/80^+$) and neutrophils ($Gr1\ Ly\text{-}6G^+$). T lymphocytes ($CD3\text{-}\varepsilon^+$) are traditionally regarded as mediating allograft rejection in conventional (nonimmune deviant) sites, and these cells were also sought.

In eyes that received subretinal transplants, the period of graft loss between POD 1 and POD 7 was characterized by infiltration of the SRS by cells expressing markers

of innate immunity (Fig. 3A). CD11b and F4/80 are cell surface markers used to identify macrophages, and Gr1 Ly-6G is a cell surface marker used to identify neutrophils. Low levels of infiltrating CD11b$^+$, F4/80$^+$, and Gr1 Ly-6G$^+$ cells were seen at POD 1 and POD 3, with a marked increase evident at POD 7. No graft cells were identified at POD 28. Only one of four eyes at POD 28 had cells remaining in the SRS, and these were F4/80$^+$ (Fig. 3Ah). No T lymphocytes (CD3-ε$^+$) were seen at each time point (Fig. 3Am–p). At POD 28, the neural retina overlying the graft site had folds in the outer nuclear layer but otherwise appeared undamaged (Fig. 3Ad, h, l, and p).

The area of immunolabeling as a function of the number of nuclei present in the SRS was calculated and expressed as μm^2/100 nuclei. A significant ($p<0.05$) increase in expression of the innate immune cell markers CD11b, F4/80, and Gr1 Ly-6G coinciding with a significant ($p<0.05$) decrease in immunolabeling of the graft cell marker (SV40T) was identified between POD 1 and POD 7 (Fig. 3B). Expression of the T-cell marker CD3-ε remained very low across all time points and was not expressed at significantly different levels between time points (Fig. 3B).

Macrophages and Neutrophils Colabel With, and Engulf, Graft Cells During the First Postoperative Week

Areas of colabeling of the graft cell marker (SV40T) with the innate immune cell markers (CD11b, F4/80, and Gr1 Ly-6G) were apparent on confocal microscopy images. The proportion of SV40T immunolabeling that colabeled with infiltrating immune cell markers on POD 1, 3, 7, and 28 was calculated. CD11b, F4/80, and Gr1 Ly-6G all colabeled with SV40T at significantly ($p<0.05$) increased levels by POD 7 (Fig. 4F). However, colabeling of SV40T with the T-lymphocyte marker (CD3-ε) remained low at all time points and did not change significantly across time points (Fig. 4F).

To better discriminate areas of colabeling, high-power z-stack confocal images were taken through these areas. SV40T immunolabeling was apparent inside the cell membranes of CD11b$^+$ (Fig. 4A) and F4/80$^+$ (Fig. 4B) cells. DIC images also identified pigment granules inside the cell membranes of these cells. Similarly, Gr1 Ly-6G$^+$/SV40T$^+$ colabeling was apparent inside cell membranes of Gr1 Ly-6G$^+$ cells (Fig. 4C–D). Reconstruction of z-stacked confocal images taken through such areas of colabeling confirms SV40T inside Gr1 Ly-6G$^+$ cells (Fig. 4E). The images presented in Figure 4 are consistent with phagocytosis of graft cells by macrophages and neutrophils.

DISCUSSION

We examined cytokine expression by DH01 RPE cells under BC and following preparation of a concentrated graft cell suspension (TC) to determine whether the graft preparation technique might influence the host immune response following transplantation. Graft preparation (TC) increased significantly the expression of almost all cytokines examined (Table 1). Notably, KC/GRO/CINC was expressed at by far the greatest levels and also demonstrated the greatest fold increase (sixfold) in expression following graft preparation. Mouse GRO and the chemoattractant KC are structural and functional homologs of the human chemokine IL-8[48]. IL-8 is a potent neutrophil chemoattractant and stimulates phagocytosis, superoxide radical production, and cytoplasmic degranulation[49,50]. Thus, production by graft cells of high levels of KC/GRO/CINC in the SRS in the period following transplantation would increase the risk of monocyte migration and inflammation at the graft site. KC/GRO/CINC, or IL-8, has not been identified previously as a potentially significant mediator of the immune response against subretinal grafts.

TC caused a threefold increase in expression of the inflammatory cytokines IL-1β, IL-5, IL-6, and IL-12. While increased expression of IL-1 and IL-6 at the graft site has been reported following human RPE xenografts to the SRS of nondystrophic Royal College of Surgeons (RCS) rats[51], the effects of these cytokines in subretinal cell transplantation are unknown. IL-1 has many proinflammatory effects including mediating a neutrophilic inflammatory response to dying cells in vivo[52]. RPE allografts to rabbits cause elevated IL-6 in the vitreous in the first week postoperatively[53]. IL-6 is a key mediator of allograft rejection, and increased expression is highly correlated with human cardiac allograft rejection[54]. Graft-produced IL-6 promotes T-cell activation and cardiac allograft rejection in the mouse[55].

DH01 expression of IL-10 increased significantly (2.1-fold increase; $p=0.024$) following graft preparation (TC) compared to baseline levels (BC). Production of IL-10 by the RPE plays a key role in modulating the posterior ocular immune microenvironment and suppressing delayed-type hypersensitivity (DTH) by diverting the immune response from a TH1- to a TH2-type immune response[56,57]. Increased IL-10 expression by DH01 RPE cells at the time of transplantation would therefore inhibit a T-lymphocytic host response against the subretinal graft.

IL-2 supports T-lymphocyte proliferation[58–62] and survival[63], as well as the differentiation of naive T lymphocytes into effector and memory T cells[64–66]. However, IL-2 also has an immunosuppressive function by promoting regulatory T cells (Tregs) production and homeostasis[67] and plays a fundamental role in immune regulation and tolerance in vivo[68–73]. While DH01 production of IL-2 increased significantly (2.7-fold increase, $p=0.002$) following graft preparation, absolute levels of IL-2 production under both BC and TC were relatively low.

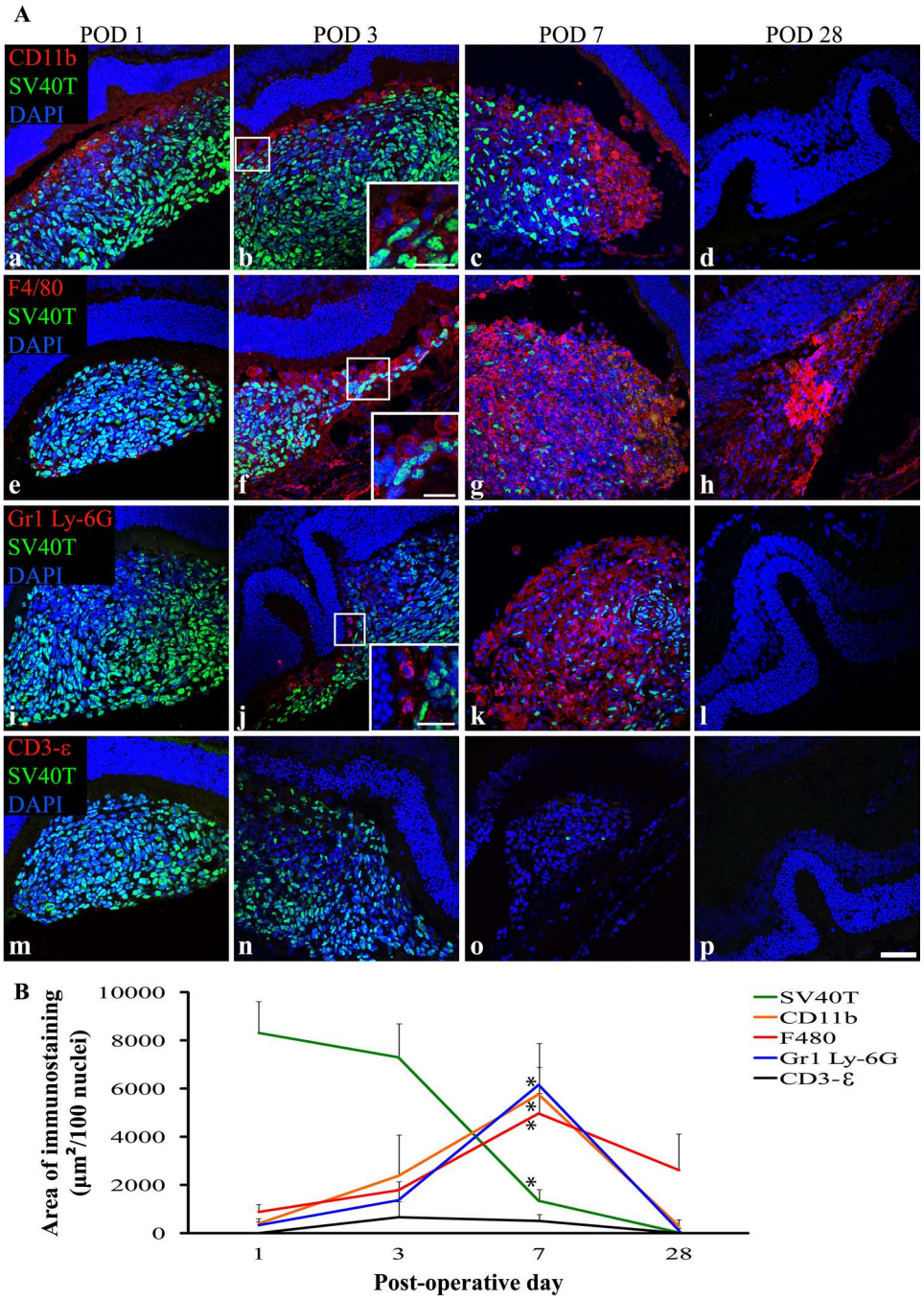

Figure 3. The period of DH01 RPE allograft loss in the SRS of healthy nonimmunosuppressed C57BL/6 mice is characterized by infiltrating cells expressing markers of macrophages (CD11b and F4/80) and neutrophils (Gr1 Ly-6G), but not by T lymphocytes (CD3-ε). (A) Representative confocal microscopy images of sections immunolabeled for SV40T (FITC, green) to identify transplanted cells, and also immunolabeled for either CD11b (a–d), F4/80 (e–h), Gr1 Ly-6G (i–l), or CD3-ε (m–p) to identify infiltrating cells (all TRITC, red). All nuclei were counterstained with DAPI (blue). At POD 1, the subretinal graft site is primarily composed of SV40T$^+$ graft cells, but by POD 7 the proportion of cells in the subretinal bolus expressing this graft cell marker has considerably decreased. CD11b$^+$ (a–c), F4/80$^+$ (e–g), and Gr1 Ly-6G$^+$ (i–k) cells infiltrate the graft in increasing numbers between POD 1 and POD 7. No graft cells are seen at POD 28 (d, h, l, p). One of four eyes assessed at POD 28 still had cells in the SRS, and these are F4/80$^+$ (h). Graft cell loss is not associated with CD3-ε$^+$ T-lymphocyte infiltration (m–p). Scale bars: 50 μm, 20 μm (high-power insets). (B) Quantitative analysis of the areas of immunolabeling confirms that the period of significant (*$p < 0.05$) graft cell loss coincides with significant (*$p < 0.05$) infiltration of the SRS by CD11b$^+$, F4/80$^+$, and Gr1 Ly-6G$^+$ cells between POD 1 and POD 7. These innate immune cells predominate over SV40T$^+$ graft cells by POD 7. CD3-ε immunolabeling remains low across all time points and does not differ significantly between time points.

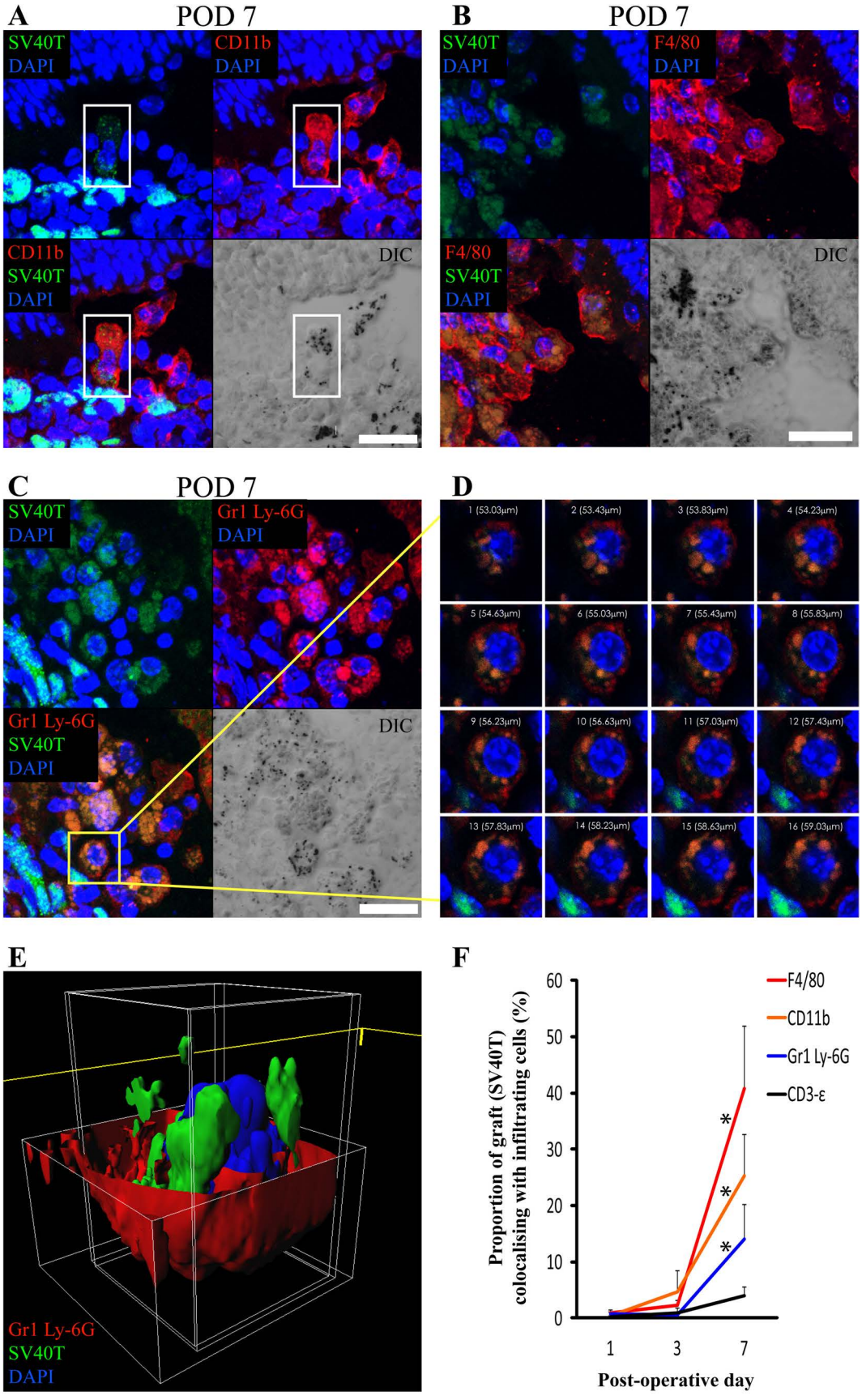
A
POD 7
SV40T
DAPI
CD11b
DAPI
CD11b
SV40T
DAPI
DIC
B
POD 7
SV40T
DAPI
F4/80
DAPI
F4/80
SV40T
DAPI
DIC
C
POD 7
SV40T
DAPI
Gr1 Ly-6G
DAPI
Gr1 Ly-6G
SV40T
DAPI
DIC
D
1 (53.03µm)
2 (53.43µm)
3 (53.83µm)
4 (54.23µm)
5 (54.63µm)
6 (55.03µm)
7 (55.43µm)
8 (55.83µm)
9 (56.23µm)
10 (56.63µm)
11 (57.03µm)
12 (57.43µm)
13 (57.83µm)
14 (58.23µm)
15 (58.63µm)
16 (59.03µm)
E
Gr1 Ly-6G
SV40T
DAPI
F
Proportion of graft (SV40T) colocalising with infiltrating cells (%)
60
50
40
30
20
10
0
1
3
7
Post-operative day
F4/80
CD11b
Gr1 Ly-6G
CD3-ε
*
*
*

In the context of consistently poor graft survival in the SRS, we sought to examine graft survival in the early postoperative period. We have previously demonstrated that our technique for preparing DH01 graft cell suspensions results in 95% cell viability at the time of transplantation[44]. Expression of SV40T by the DH01 cell line enabled examination of the fate of transplanted cells during the first postoperative month. The proportion of the subretinal bolus composed of grafted cells reduced from 90% on POD 3 to just 20% on POD 7, and no grafted cells survived to POD 28 (Fig. 2).

Our finding of rapid graft loss in the SRS is consistent with other studies. Human RPE cells xenografted into the SRS of cyclosporine-immunosuppressed RCS rats are quickly lost with just 27% survival at POD 7 and 11% at POD 28[28]. Similarly, just 3% of subretinal porcine fetal RPE cells xenografted into rabbits survived to 1 month in immunocompetent animals, and only 10.5% survived in rabbits receiving daily triple systemic immunosuppressive therapy with prednisone, cyclosporine, and azathioprine[29].

In contrast to solid tissue or organ transplants, cell transplants are commonly derived from cell cultures and delivered as a cell suspension (e.g., stem cells[74], Schwann cells[75,76], pancreatic islets[43], and RPE cells[8,18,20]). Transplantation paradigms involving cell suspension grafts have poor rates of graft survival. Human fetal dopaminergic neuronal xenografts to cyclosporine-immunosuppressed rats had only 5%–6% survival[77], and poor graft survival is also a feature of fetal nigral allografts in humans[78,79].

TUNEL labeling identifies apoptotic cells by detecting DNA fragmentation. However, necrosis is also accompanied by DNA breaks, and thus TUNEL labeling also identifies necrotic cells[80–82]. It is unlikely that the rapid graft cell loss observed in this study was due to apoptosis or necrosis, as rates of TUNEL labeling of grafted cells remained low at all time points (Fig. 2A). Graft cell apoptosis/necrosis was just 2% at POD 1, <1% at POD 3, and 5% at POD 7 (Fig. 2C). We hypothesized that the rapid graft cell loss observed during the first postoperative week was a consequence of a host innate immune response against the subretinal allograft.

On POD 1 and POD 3, 90% of cells in the SRS were identifiable as graft cells ($SV40T^+$). However, by POD 7 this figure reduced to just 20% (Fig. 2C). Thus, the remaining 80% of cells at this time must be host derived. We characterized the cellular composition of the subretinal bolus during the first postoperative month and found that macrophages (CD11b and F4/80) infiltrated subretinal grafts on POD 1 and POD 3 and predominated over transplanted cells by POD 7 (Fig. 3Aa–h and B).

There was also a significant increase ($p<0.05$) in immunohistochemical colabeling of the graft cell marker (SV40T) with macrophages (CD11b and F4/80) at POD 7 (Fig. 4F). High-power images of areas of colabeling confirmed the presence of the graft cell marker inside macrophages (Fig. 4A and B). Thus, we have confirmed that macrophages not only associate with subretinal allografts but also engulf transplanted cells.

The interaction of graft cells with $F4/80^+$ macrophages in the SRS is particularly interesting because the mouse macrophage F4/80 receptor is known to play a critical role in the generation of antigen-specific efferent Tregs that suppress antigen-specific DTH responses[83]. However, while $F4/80^+$ macrophages may inhibit a T-lymphocytic adaptive immune response, our observations reveal direct engulfment of transplanted cells by $F4/80^+$ macrophages. Macrophages have been reported to associate with

FACING PAGE

Figure 4. Colabeling of DH01 allografts with infiltrating $CD11b^+$, $F4/80^+$, and Gr1 Ly-$6G^+$ cells peaks at POD 7 with evidence of graft engulfment by these innate immune cells. Large areas of SV40T were observed to colabel with $CD11b^+$, $F4/80^+$, and Gr1 Ly-$6G^+$ on POD 7. Colabeling of SV40T with the T-lymphocyte marker (CD3-ε) remained low at all time points. Representative images of the immunofluorescence colabeling evident on POD 7 are shown. (A) The highlighted cell (white box) in the center of this image has positive cell membrane immunolabeling for the macrophage marker CD11b (TRITC, red) on POD 7. SV40T (FITC, green) immunolabeling can be seen within this $CD11b^+$ cell, suggesting engulfment of graft by the macrophage. The differential interference contrast (DIC) image also identifies pigment granules within $CD11b^+$ cells. Scale bar: 20 μm. (B) Multiple cells in this image have cell membrane immunolabeling for the macrophage marker F4/80 (TRITC, red) on POD 7. SV40T (FITC, green) immunolabeling can be seen within these $F4/80^+$ cells. Areas of $F4/80^+/SV40T^+$ colabeling (orange) suggest graft engulfment by macrophages. The DIC image also identifies pigment granules within $F4/80^+$ cells. Scale bar: 20 μm. (C) Many cells in this POD 7 subretinal graft have immunofluorescence colabeling (orange) for Gr1 Ly-6G (TRITC, red) and SV40T (FITC, green). Scale bar: 10 μm. (D) Sequential single optical sections from the z-stack confocal image through the highlighted (yellow box) Gr1 Ly-$6G^+$ neutrophil on POD 7 is consistent with phagocytosis of SV40T from the neutrophil cell membrane. (E) The z-stack confocal image of the cell highlighted in (C) was also reconstructed in three-dimensional (3D) form, and the red channel was removed from the top portion of the cell to enable visualization inside the cell membrane. The reconstructed image confirms the presence of graft (SV40T, green) inside the neutrophil cell membrane (Gr1 Ly-6G, red). (F) The proportions of SV40T that colabeled with CD11b, F4/80, Gr1 Ly-6G, and CD3-ε were analyzed. Colabeling of SV40T with all infiltrating immune cell markers was minimal on POD 1 and POD 3. However, there was a significant ($*p<0.05$) increase in the proportion of the graft (SV40T) that colabeled with F4/80, CD11b, and Gr1 Ly-6G between POD 1 and POD 7. Colabeling of SV40T with the T-lymphocyte marker (CD3-ε) remained low at all time points, and there was no statistically significant difference in SV40T/CD3-ε colabeling between time points.

subretinal grafts in many host species including the mouse[84], rat[14,26,27], rabbit[29–31,85–87], pig[88], and primate[6]. While these studies reported macrophages associating with subretinal grafts, they did not correlate macrophage infiltration with graft cell loss. The study presented is the first investigation to make this connection.

The observation of positive immunolabeling for F4/80, but not for CD11b, in the ganglion cell layer was unexpected and may be a consequence of the particularly high levels of expression of F4/80 by ameboid ganglion cell layer microglia compared to ramified parenchymal microglia[89]. Although the immunofluorescence techniques employed in this study were insufficient to detect the CD11b antigens expressed by ganglion cell layer microglia, they clearly identified CD11b cells in the SRS.

Zecher et al. described an innate immune response to allografts mediated by macrophages that is independent of natural killer cells and T lymphocytes[90]. Graft survival in the early postoperative period is promoted by macrophage inhibition in cellular transplants of pancreatic islet cells[91] and spleen cells[92]. Macrophage depletion via subconjunctival administration of clodronate liposomes also promotes long-term survival of high-risk corneal grafts[93]. We observed a significant macrophage response in the subretinal graft coinciding with the period of graft cell loss during the first postoperative week. It is likely that perioperative macrophage depletion or inhibition may also prove useful in promoting subretinal graft survival.

Having found that DH01 cells prepared for transplantation expressed large amounts of the neutrophil chemoattractant KC/GRO/CINC, we also investigated whether neutrophils infiltrated the subretinal graft. We used an antibody against Gr1 Ly-6G, which detects the myeloid differentiation antigen Gr1[94] and specifically identifies neutrophils as distinct from monocyte–macrophages via Ly-6G[95]. We found a significant increase in Gr1 Ly-6G$^+$ cells infiltrating the subretinal cell bolus during the first postoperative week (Fig. 3Ai–k and B). Moreover, by POD 7 there was also a significant increase in immunofluorescence colabeling of transplanted cells with this neutrophil cell marker (Fig. 4F). The 3D image reconstruction of areas of colabeling demonstrated the presence of the graft cell marker internal to the neutrophil cell membrane confirming engulfment of graft cells by infiltrating neutrophils (Fig. 4C–E). Neutrophils have not previously been identified in subretinal grafts.

Neutrophils have recently been implicated as mediators of cardiac graft failure. They are the first leukocyte to infiltrate cardiac allografts, arriving within 1 h following transplantation[96]. Neutrophil infiltration also correlates with cardiac allograft rejection severity[97], and cardiac allograft survival is promoted by neutrophil depletion[98] and inhibition of neutrophil infiltration[99]. Statins inhibit neutrophil transendothelial migration[100,101], and when used in patients with cardiac allografts they lower the incidence of cardiac allograft vasculopathy and reduce the severity of allograft rejection[102,103]. Thus, the use of perioperative statins may also prove beneficial in suppressing neutrophil infiltration and in promoting subretinal graft survival.

T-lymphocyte (CD3-ε) infiltration was not a feature of this study (Fig. 3Am–p and B). T lymphocytes have also been notable by their absence in subretinal transplants to the rat[26,27], rabbit[29–31,85–87], and pig[88]. This is consistent with the deviant immune environment of the SRS[32–34] characterized by a suppressed T-lymphocytic adaptive immune response[35,36,104,105]. Interestingly, after finding no significant differences between cyclosporine-immunosuppressed and control animals in RPE cell suspension allografts in the rabbit, Crafoord et al. concluded that graft failure was caused by either immunological mechanisms not inhibited by cyclosporine or by nonimmunologic events[31]. The study presented here describes the cellular infiltrate in the SRS at specific time points following subretinal allograft transplantation. It is possible that a T-lymphocyte response was occurring at the regional lymph nodes; however, this possibility was not investigated. Nevertheless, we found that the majority of graft cell loss had occurred by POD 7. This is much earlier than acute allograft rejection mediated by T lymphocytes, which occurs at 10–13 days following transplantation[106].

Lopez et al. suggested that RPE cells transplanted to the SRS of the RCS rat could phagocytize shed outer segments[7]. This conclusion was made because histology showed pigmented cells incorporated into the host RPE layer, in the SRS, and also in between photoreceptor outer segments. These cells were assumed to be transplanted cells. However, the electron microscopy images revealed 10 times as many phagosomes in the putative transplanted RPE cells compared to normal rat RPE cells. The staining and imaging techniques were insufficient to determine if the phagosomes seen were truly in transplanted RPE cells or another cell type. In the present study, the DIC images clearly demonstrate pigment granules in macrophages (Fig. 4A and B) and neutrophils (Fig. 4C). We propose that infiltrating macrophages and neutrophils, rather than transplanted RPE cells, may be responsible for the hyperphagocytosis observed by Lopez et al.

Retinal detachment activates retinal microglia[107]. We observed a considerable infiltrate of macrophages that appeared to arrive from the retinal side of the subretinal graft (Fig. 3Aa, b, and f). It is possible that the macrophage infiltration represented activated retinal microglia as CD11b[108] and F4/80[109] also identify retinal microglia. The macrophage or microglial response we observed was likely exaggerated due to the high-density cell suspension graft delivered. However, it is conceivable that a low-density cell suspension graft or even a simple subretinal

injection of saline may result in lower levels of microglia activation and subretinal infiltration that proves beneficial to the host. Activated retinal microglia may assume a phagocytic phenotype and migrate to the SRS, thereby adopting the role of outer segment phagocytosis and enabling photoreceptor rescue. This explanation would theoretically explain the following phenomena of subretinal transplantation observed particularly, though not exclusively, in the RCS rat: (1) transplantation of many different cell types to the SRS results in photoreceptor rescue[14–16,76,110]; (2) sham surgery has anatomical[76,111] and functional benefits[18–21], and even subretinal saline alone promotes photoreceptor survival[112]; (3) the area of rescue may extend beyond the area of the graft[17]; (4) macrophages or macrophage-like cells have repeatedly been seen at the graft site[6,14,26,27,29–31,84–88]; and (5) temporal photoreceptor rescue may outlast graft survival[18].

Our observation of infiltrating cells expressing the neutrophil marker Gr1 Ly-6G is novel. Neutrophils are distinguished from monocyte–macrophages via their expression of Ly-6G[95]. Neutrophils in the eye are $CD11b^+$/Gr1 Ly-$6G^{+}$[113]. However, neutrophils are negative for F4/80[114]. It follows therefore that the $CD11b^+$ cellular infiltrate observed during the first week following transplantation in the present study may comprise a combination of $CD11b^+$/$F4/80^+$/Gr1 Ly-$6G^-$ microglia and $CD11b^+$/$F4/80^-$/Gr1 Ly-$6G^+$ neutrophils. However, the immunohistochemical methods in our study could not subclassify the cellular infiltrate with certainty. Further studies such as multilabeled flow cytometric analysis of cells extracted from the SRS, or following whole-eye dissociation, would be helpful in more precisely phenotyping the infiltrate. Nevertheless, the data presented here reveal, for the first time, a critical role for the innate immune system early in subretinal graft rejection, while T lymphocytes did not feature at all during the main period of graft loss (PODs 3–7).

The rapid loss of graft cells observed in this study was accompanied by comparatively very low levels of graft cell death as examined by TUNEL labeling (Fig. 2A and C). TUNEL labeling identifies apoptotic and necrotic cells by detecting DNA strand breaks[80–82]. However, it is possible that the graft cell loss observed in the present study occurred via a process other than apoptosis or necrosis, such as by autophagy[115,116]. Autophagic cell death is characterized by increased autophagosomes/autolysosomes and extensive cytoplasmic vacuolization, but with relatively minor changes to the nucleus and chromatin[117]. Therefore, this mode of cell death could remain undetected by TUNEL labeling. Autophagic cell death is triggered by stresses including nutrient deprivation[118–121] and hypoxia[119]. In order to limit potential immunological triggers against subretinal cell suspension transplants, such grafts are normally delivered suspended in serum-free medium[18,20,76]. For this reason, we also suspended DH01 cells in serum-free medium immediately prior to transplantation. It may be that the stresses of serum deprivation and the other processes involved in preparing a highly concentrated graft cell suspension (TC) trigger autophagic graft cell death. Cells that undergo autophagic cell death may be cleared by phagocytosis[122–124] in a process that limits inflammatory and immunological responses[125]. Consistent with these features of autophagic cell death, there was clear evidence of graft engulfment by macrophages and neutrophils in this study (Fig. 4), and the retina overlying the graft site remained remarkably preserved with no substantial evidence of inflammatory scarring at POD 28 (Fig. 3Ad, h, l, and p).

Toll-like receptors (TLRs) are phylogenetically ancient mediators of innate immunity that detect microbes via pathogen-associated molecular patterns (PAMPs)[38,126]. Stressed and dying cells express endogenous TLR ligands termed damage-associated molecular patterns (DAMPs)[127]. Activation of the innate immune system via TLRs plays an important role in allograft rejection[39,40]. Blocking TLR4-mediated graft rejection prolongs pancreatic islet cell transplant survival[43]. TLR4 is constitutively expressed by RPE cells[128,129], photoreceptors[130], and resident antigen-presenting cells in the normal human uveal tract[131]. However, there have been no studies to date regarding the role of TLRs in subretinal cell transplantation. Cell suspension grafts are exposed to many potential stressors including enzymatic cleavage, centrifugation, resuspension in serum-free medium, and delivery through nonbiological injectors. It is likely that these processes not only incite increased inflammatory cytokine and chemokine production by graft cells as demonstrated in this study but may also provoke increased expression of DAMPs. Following transplantation to the SRS, excessive DAMP expression by transplanted cells could propagate an innate immune response by binding host TLRs, thereby triggering host cytokine and chemokine expression capable of recruiting microglia/macrophages from the overlying retina as well as neutrophils from the circulation. DAMPs may also trigger complement activation[132,133] and the release of anaphylatoxins capable of mediating leukocyte chemotaxis[134,135].

Future strategies to suppress the host immune response against cells transplanted to the SRS should focus more on limiting the effect of infiltrating macrophages and neutrophils by specifically targeting these mediators of the innate immune response. Potential agents include clodronate[91,93], statins[102,103], resveratrol[136,137], and minocycline[138,139]. Controlling innate immune and inflammatory responses following transplantation will be particularly important in the context of treating conditions such as age-related macular degeneration, which is characterized by increased macrophage infiltration at the affected site[140–142].

The rapid innate immune response observed in our study is likely a consequence of multiple inciting factors including increased expression of inflammatory cytokines and DAMPs by cells prepared for transplantation. Such factors are independent of genetic mismatch and would not be restricted to allogeneic cell transplants. Consequently, the innate immune response observed in our study is also likely to occur in response to other cell transplants including syngeneic, autologous, and stem cell transplants. The future success of subretinal transplantation will require more emphasis to be placed on optimizing techniques to prepare and deliver grafts of high quality that limit rapid innate immune-mediated clearance of transplanted cells. Furthermore, pharmacological strategies in the field of subretinal transplantation must go beyond merely suppressing adaptive immunity in the host and focus on methods of inhibiting the early innate immune response.

ACKNOWLEDGMENTS: This work was funded by the Health Research Board, Ireland (project grant RP/2007/202), and by an Irish College of Ophthalmologists Fellowship awarded to Kevin Kennelly, Ph.D. The funders had no role in the study design, data collection and analysis, decision to publish, or preparation of the manuscript. The authors are grateful for the assistance provided with the confocal microscopy and image analysis sections of this study by Orla Hanrahan, Ph.D., and Gavin McManus, Ph.D., at the Microscopy and Imaging Facility at the School of Biochemistry and Immunology, Trinity College Dublin, Ireland. The authors also appreciate the assistance provided with statistical analysis by Timothy Grant, C.Stat., C.Sci., and Ricardo Segurado, Ph.D., at the Centre for Support and Training in Analysis and Research, University College Dublin, Ireland. The authors declare no conflicts of interest.

REFERENCES

1. Resnikoff S, Pascolini D, Etya'ale D, Kocur I, Pararajasegaram R, Pokharel GP, Mariotti SP. Global data on visual impairment in the year 2002. Bull World Health Organ. 2004;82(11):844–51.
2. Rosenfeld PJ, Brown DM, Heier JS, Boyer DS, Kaiser PK, Chung CY, Kim RY. Ranibizumab for neovascular age-related macular degeneration. N Engl J Med. 2006; 355(14):1419–31.
3. Brown DM, Kaiser PK, Michels M, Soubrane G, Heier JS, Kim RY, Sy JP, Schneider S. Ranibizumab versus verteporfin for neovascular age-related macular degeneration. N Engl J Med. 2006;355(14):1432–44.
4. Gragoudas ES, Adamis AP, Cunningham ET Jr, Feinsod M, Guyer DR. Pegaptanib for neovascular age-related macular degeneration. N Engl J Med. 2004;351(27):2805–16.
5. Lee PP, Feldman ZW, Ostermann J, Brown DS, Sloan FA. Longitudinal prevalence of major eye diseases. Arch Ophthalmol. 2003;121(9):1303–10.
6. Gouras P, Flood MT, Kjedbye H, Bilek MK, Eggers H. Transplantation of cultured human retinal epithelium to Bruch's membrane of the owl monkey's eye. Curr Eye Res. 1985;4(3):253–65.
7. Lopez R, Gouras P, Kjeldbye H, Sullivan B, Reppucci V, Brittis M, Wapner F, Goluboff E. Transplanted retinal pigment epithelium modifies the retinal degeneration in the RCS rat. Invest Ophthalmol Vis Sci. 1989;30(3): 586–8.
8. Li LX, Turner JE. Inherited retinal dystrophy in the RCS rat: Prevention of photoreceptor degeneration by pigment epithelial cell transplantation. Exp Eye Res. 1988; 47(6):911–7.
9. Gouras P, Lopez R, Kjeldbye H, Sullivan B, Brittis M. Transplantation of retinal epithelium prevents photoreceptor degeneration in the RCS rat. Prog Clin Biol Res. 1989;314:659–71.
10. Durlu YK, Tamai M. Transplantation of retinal pigment epithelium using viable cryopreserved cells. Cell Transplant. 1997;6(2):149–62.
11. Lavail MM, Li L, Turner JE, Yasumura D. Retinal pigment epithelial cell transplantation in RCS rats: Normal metabolism in rescued photoreceptors. Exp Eye Res. 1992;55(4):555–62.
12. Lin N, Fan W, Sheedlo HJ, Aschenbrenner JE, Turner JE. Photoreceptor repair in response to RPE transplants in RCS rats: Outer segment regeneration. Curr Eye Res. 1996;15(10):1069–77.
13. Phillips SJ, Sadda SR, Tso MO, Humayan MS, de Juan E Jr, Binder S. Autologous transplantation of retinal pigment epithelium after mechanical debridement of Bruch's membrane. Curr Eye Res. 2003;26(2):81–8.
14. Jiang LQ, Hamasaki D. Corneal electroretinographic function rescued by normal retinal pigment epithelial grafts in retinal degenerative Royal College of Surgeons rats. Invest Ophthalmol Vis Sci. 1994;35(13):4300–9.
15. Sauve Y, Lu B, Lund RD. The relationship between full field electroretinogram and perimetry-like visual thresholds in RCS rats during photoreceptor degeneration and rescue by cell transplants. Vision Res. 2004;44(1): 9–18.
16. Sauve Y, Pinilla I, Lund RD. Partial preservation of rod and cone ERG function following subretinal injection of ARPE-19 cells in RCS rats. Vision Res. 2006; 46(8–9):1459–72.
17. Sauve Y, Klassen H, Whiteley SJ, Lund RD. Visual field loss in RCS rats and the effect of RPE cell transplantation. Exp Neurol. 1998;152(2):243–50.
18. Lund RD, Adamson P, Sauve Y, Keegan DJ, Girman SV, Wang S, Winton H, Kanuga N, Kwan AS, Beauchene L, Zerbib A, Hetherington L, Couraud PO, Coffey P, Greenwood J. Subretinal transplantation of genetically modified human cell lines attenuates loss of visual function in dystrophic rats. Proc Natl Acad Sci USA 2001; 98(17):9942–7.
19. Sauve Y, Girman SV, Wang S, Keegan DJ, Lund RD. Preservation of visual responsiveness in the superior colliculus of RCS rats after retinal pigment epithelium cell transplantation. Neuroscience 2002;114(2):389–401.
20. Coffey PJ, Girman S, Wang SM, Hetherington L, Keegan DJ, Adamson P, Greenwood J, Lund RD. Long-term preservation of cortically dependent visual function in RCS rats by transplantation. Nat Neurosci. 2002;5(1):53–6.
21. Girman SV, Wang S, Lund RD. Cortical visual functions can be preserved by subretinal RPE cell grafting in RCS rats. Vision Res. 2003;43(17):1817–27.
22. Whiteley SJ, Litchfield TM, Coffey PJ, Lund RD. Improvement of the pupillary light reflex of Royal College of Surgeons rats following RPE cell grafts. Exp Neurol. 1996;140(1):100–4.

23. Binder S, Krebs I, Hilgers RD, Abri A, Stolba U, Assadoulina A, Kellner L, Stanzel BV, Jahn C, Feichtinger H. Outcome of transplantation of autologous retinal pigment epithelium in age-related macular degeneration: A prospective trial. Invest Ophthalmol Vis Sci. 2004;45(11):4151–60.
24. Falkner-Radler CI, Krebs I, Glittenberg C, Povazay B, Drexler W, Graf A, Binder S. Human retinal pigment epithelium (RPE) transplantation: Outcome after autologous RPE-choroid sheet and RPE cell-suspension in a randomised clinical study. Br J Ophthalmol. 2011; 95(3):370–5.
25. Schwartz SD, Hubschman JP, Heilwell G, Franco-Cardenas V, Pan CK, Ostrick RM, Mickunas E, Gay R, Klimanskaya I, Lanza R. Embryonic stem cell trials for macular degeneration: A preliminary report. Lancet 2012; 379(9817):713–20.
26. Grisanti S, Szurman P, Jordan J, Kociok N, Bartz-Schmidt KU, Heimann K. Xenotransplantation of retinal pigment epithelial cells into RCS rats. Jpn J Ophthalmol. 2002; 46(1):36–44.
27. Zhang X, Bok D. Transplantation of retinal pigment epithelial cells and immune response in the subretinal space. Invest Ophthalmol Vis Sci. 1998;39(6):1021–7.
28. Wang S, Lu B, Wood P, Lund RD. Grafting of ARPE-19 and Schwann cells to the subretinal space in RCS rats. Invest Ophthalmol Vis Sci. 2005;46(7):2552–60.
29. Del Priore LV, Ishida O, Johnson EW, Sheng Y, Jacoby DB, Geng L, Tezel TH, Kaplan HJ. Triple immune suppression increases short-term survival of porcine fetal retinal pigment epithelium xenografts. Invest Ophthalmol Vis Sci. 2003;44(9):4044–53.
30. Crafoord S, Algvere PV, Seregard S, Kopp ED. Long-term outcome of RPE allografts to the subretinal space of rabbits. Acta Ophthalmol Scand. 1999;77(3):247–54.
31. Crafoord S, Algvere PV, Kopp ED, Seregard S. Cyclosporine treatment of RPE allografts in the rabbit subretinal space. Acta Ophthalmol Scand. 2000;78(2):122–9.
32. Jiang LQ, Jorquera M, Streilein JW. Subretinal space and vitreous cavity as immunologically privileged sites for retinal allografts. Invest Ophthalmol Vis Sci. 1993; 34(12):3347–54.
33. Wenkel H, Streilein JW. Analysis of immune deviation elicited by antigens injected into the subretinal space. Invest Ophthalmol Vis Sci. 1998;39(10):1823–34.
34. Gregerson DS, Dou C. Spontaneous induction of immunoregulation by an endogenous retinal antigen. Invest Ophthalmol Vis Sci. 2002;43(9):2984–91.
35. Farrokh-Siar L, Rezai KA, Semnani RT, Patel SC, Ernest JT, Peterson EJ, Koretzky GA, van Seventer GA. Human fetal retinal pigment epithelial cells induce apoptosis in the T-cell line Jurkat. Invest Ophthalmol Vis Sci. 1999;40(7):1503–11.
36. Willermain F, Caspers-Velu L, Nowak B, Stordeur P, Mosselmans R, Salmon I, Velu T, Bruyns C. Retinal pigment epithelial cells phagocytosis of T lymphocytes: Possible implication in the immune privilege of the eye. Br J Ophthalmol. 2002;86(12):1417–21.
37. Li X, Tupper JC, Bannerman DD, Winn RK, Rhodes CJ, Harlan JM. Phosphoinositide 3 kinase mediates Toll-like receptor 4-induced activation of NF-kappa B in endothelial cells. Infect Immun. 2003;71(8):4414–20.
38. Medzhitov R. Recognition of microorganisms and activation of the immune response. Nature 2007;449(7164): 819–26.
39. Paul LC. Current knowledge of the pathogenesis of chronic allograft dysfunction. Transplant Proc. 1999;31(4):1793–5.
40. LaRosa DF, Rahman AH, Turka LA. The innate immune system in allograft rejection and tolerance. J Immunol. 2007;178(12):7503–9.
41. Land WG. Innate immunity-mediated allograft rejection and strategies to prevent it. Transplant Proc. 2007; 39(3):667–72.
42. Goldstein DR, Tesar BM, Akira S, Lakkis FG. Critical role of the Toll-like receptor signal adaptor protein MyD88 in acute allograft rejection. J Clin Invest. 2003; 111(10):1571–8.
43. Goldberg A, Parolini M, Chin BY, Czismadia E, Otterbein LE, Bach FH, Wang H. Toll-like receptor 4 suppression leads to islet allograft survival. FASEB J. 2007;21(11):2840–8.
44. Kennelly KP, Wallace DM, Holmes TM, Hankey DJ, Grant TS, O'Farrelly C, Keegan DJ. Preparation of preconfluent retinal cells increases graft viability in vitro and in vivo: A mouse model. PLoS One 2011;6(6):e21365.
45. Croxford JL, Triantaphyllopoulos KA, Neve RM, Feldmann M, Chernajovsky Y, Baker D. Gene therapy for chronic relapsing experimental allergic encephalomyelitis using cells expressing a novel soluble p75 dimeric TNF receptor. J Immunol. 2000;164(5):2776–81.
46. Almazan G, McKay R. An oligodendrocyte precursor cell line from rat optic nerve. Brain Res. 1992;579(2): 234–45.
47. Wallace DM, Donovan M, Cotter TG. Histone deacetylase activity regulates apaf-1 and caspase 3 expression in the developing mouse retina. Invest Ophthalmol Vis Sci. 2006;47(7):2765–72.
48. Himi T, Yoshioka I, Kataura A. Production and gene expression of IL-8-like cytokine GRO/CINC-1 in rat nasal mucosa. Acta Otolaryngol. 1997;117(1):123–7.
49. Harada A, Sekido N, Akahoshi T, Wada T, Mukaida N, Matsushima K. Essential involvement of interleukin-8 (IL-8) in acute inflammation. J Leukoc Biol. 1994;56(5): 559–64.
50. Sekido N, Mukaida N, Harada A, Nakanishi I, Watanabe Y, Matsushima K. Prevention of lung reperfusion injury in rabbits by a monoclonal antibody against interleukin-8. Nature 1993;365(6447):654–7.
51. Abe T, Takeda Y, Yamada K, Akaishi K, Tomita H, Sato M, Tamai M. Cytokine gene expression after subretinal transplantation. Tohoku J Exp Med. 1999;189(3):179–89.
52. Chen CJ, Kono H, Golenbock D, Reed G, Akira S, Rock KL. Identification of a key pathway required for the sterile inflammatory response triggered by dying cells. Nat Med. 2007;13(7):851–6.
53. Enzmann V, Faude F, Wiedemann P, Kohen L. The local and systemic secretion of the pro-inflammatory cytokine interleukin-6 after transplantation of retinal pigment epithelium cells in a rabbit model. Curr Eye Res. 2000;21(1):530–4.
54. Zhao XM, Frist WH, Yeoh TK, Miller GG. Expression of cytokine genes in human cardiac allografts: Correlation of IL-6 and transforming growth factor-beta (TGF-beta) with histological rejection. Clin Exp Immunol. 1993;93(3):448–51.
55. Liang Y, Christopher K, Finn PW, Colson YL, Perkins DL. Graft produced interleukin-6 functions as a danger signal and promotes rejection after transplantation. Transplantation 2007;84(6):771–7.

56. D'Orazio TJ, Niederkorn JY. A novel role for TGF-beta and IL-10 in the induction of immune privilege. J Immunol. 1998;160(5):2089–98.
57. Streilein JW. Ocular immune privilege: Therapeutic opportunities from an experiment of nature. Nat Rev Immunol. 2003;3(11):879–89.
58. Bamford RN, Grant AJ, Burton JD, Peters C, Kurys G, Goldman CK, Brennan J, Roessler E, Waldmann TA. The interleukin (IL) 2 receptor beta chain is shared by IL-2 and a cytokine, provisionally designated IL-T, that stimulates T-cell proliferation and the induction of lymphokine-activated killer cells. Proc Natl Acad Sci USA 1994;91(11):4940–4.
59. Gillis S, Baker PE, Ruscetti FW, Smith KA. Long-term culture of human antigen-specific cytotoxic T-cell lines. J Exp Med. 1978;148(4):1093–8.
60. Morgan DA, Ruscetti FW, Gallo R. Selective in vitro growth of T lymphocytes from normal human bone marrows. Science 1976;193(4257):1007–8.
61. Smith KA. Interleukin-2: Inception, impact, and implications. Science 1988;240(4856):1169–76.
62. Smith KA, Gilbride KJ, Favata MF. Lymphocyte activating factor promotes T-cell growth factor production by cloned murine lymphoma cells. Nature 1980;287(5785): 853–5.
63. Blattman JN, Grayson JM, Wherry EJ, Kaech SM, Smith KA, Ahmed R. Therapeutic use of IL-2 to enhance antiviral T-cell responses in vivo. Nat Med. 2003;9(5):540–7.
64. Cho JH, Boyman O, Kim HO, Hahm B, Rubinstein MP, Ramsey C, Kim DM, Surh CD, Sprent J. An intense form of homeostatic proliferation of naive CD8+ cells driven by IL-2. J Exp Med. 2007;204(8):1787–801.
65. Kamimura D, Bevan MJ. Naive CD8+ T cells differentiate into protective memory-like cells after IL-2 anti IL-2 complex treatment in vivo. J Exp Med. 2007;204(8):1803–12.
66. Ke Y, Ma H, Kapp JA. Antigen is required for the activation of effector activities, whereas interleukin 2 is required for the maintenance of memory in ovalbumin-specific, CD8+ cytotoxic T lymphocytes. J Exp Med. 1998;187(1):49–57.
67. Laurence A, Tato CM, Davidson TS, Kanno Y, Chen Z, Yao Z, Blank RB, Meylan F, Siegel R, Hennighausen L, Shevach EM, O'shea JJ. Interleukin-2 signaling via STAT5 constrains T helper 17 cell generation. Immunity 2007;26(3):371–81.
68. D'Cruz LM, Klein L. Development and function of agonist-induced CD25+Foxp3+ regulatory T cells in the absence of interleukin 2 signaling. Nat Immunol. 2005;6(11):1152–9.
69. Fontenot JD, Rasmussen JP, Gavin MA, Rudensky AY. A function for interleukin 2 in Foxp3-expressing regulatory T cells. Nat Immunol. 2005;6(11):1142–51.
70. Klebb G, Autenrieth IB, Haber H, Gillert E, Sadlack B, Smith KA, Horak I. Interleukin-2 is indispensable for development of immunological self-tolerance. Clin Immunol Immunopathol. 1996;81(3):282–6.
71. Papiernik M, de Moraes ML, Pontoux C, Vasseur F, Penit C. Regulatory CD4 T cells: Expression of IL-2R alpha chain, resistance to clonal deletion and IL-2 dependency. Int Immunol. 1998;10(4):371–8.
72. Suzuki H, Zhou YW, Kato M, Mak TW, Nakashima I. Normal regulatory alpha/beta T cells effectively eliminate abnormally activated T cells lacking the interleukin 2 receptor beta in vivo. J Exp Med. 1999;190(11):1561–72.
73. Wolf M, Schimpl A, Hunig T. Control of T cell hyperactivation in IL-2-deficient mice by CD4(+)CD25(-) and CD4(+)CD25(+) T cells: Evidence for two distinct regulatory mechanisms. Eur J Immunol. 2001;31(6):1637–45.
74. Young MJ, Ray J, Whiteley SJ, Klassen H, Gage FH. Neuronal differentiation and morphological integration of hippocampal progenitor cells transplanted to the retina of immature and mature dystrophic rats. Mol Cell Neurosci. 2000;16(3):197–205.
75. Hill CE, Hurtado A, Blits B, Bahr BA, Wood PM, Bartlett Bunge M, Oudega M. Early necrosis and apoptosis of Schwann cells transplanted into the injured rat spinal cord. Eur J Neurosci. 2007;26(6):1433–45.
76. Keegan DJ, Kenna P, Humphries MM, Humphries P, Flitcroft DI, Coffey PJ, Lund RD, Lawrence JM. Transplantation of syngeneic Schwann cells to the retina of the rhodopsin knockout (rho(-/-)) mouse. Invest Ophthalmol Vis Sci. 2003;44(8):3526–32.
77. Frodl EM, Duan WM, Sauer H, Kupsch A, Brundin P. Human embryonic dopamine neurons xenografted to the rat: Effects of cryopreservation and varying regional source of donor cells on transplant survival, morphology and function. Brain Res. 1994;647(2):286–98.
78. Kordower JH, Rosenstein JM, Collier TJ, Burke MA, Chen EY, Li JM, Martel L, Levey AE, Mufson EJ, Freeman TB, Olanow CW. Functional fetal nigral grafts in a patient with Parkinson's disease: Chemoanatomic, ultrastructural, and metabolic studies. J Comp Neurol. 1996;370(2):203–30.
79. Kordower JH, Freeman TB, Chen EY, Mufson EJ, Sanberg PR, Hauser RA, Snow B, Olanow CW. Fetal nigral grafts survive and mediate clinical benefit in a patient with Parkinson's disease. Mov Disord. 1998;13(3):383–93.
80. Charriaut-Marlangue C, Ben-Ari Y. A cautionary note on the use of the TUNEL stain to determine apoptosis. Neuroreport 1995;7(1):61–4.
81. Yasuda M, Umemura S, Osamura RY, Kenjo T, Tsutsumi Y. Apoptotic cells in the human endometrium and placental villi: Pitfalls in applying the TUNEL method. Arch Histol Cytol. 1995;58(2):185–90.
82. Kelly KJ, Sandoval RM, Dunn KW, Molitoris BA, Dagher PC. A novel method to determine specificity and sensitivity of the TUNEL reaction in the quantitation of apoptosis. Am J Physiol Cell Physiol. 2003;284(5):C1309–18.
83. Lin HH, Faunce DE, Stacey M, Terajewicz A, Nakamura T, Zhang-Hoover J, Kerley M, Mucenski ML, Gordon S, Stein-Streilein J. The macrophage F4/80 receptor is required for the induction of antigen-specific efferent regulatory T cells in peripheral tolerance. J Exp Med. 2005;201(10):1615–25.
84. Jiang LQ, Jorquera M, Streilein JW. Immunologic consequences of intraocular implantation of retinal pigment epithelial allografts. Exp Eye Res. 1994;58(6):719–28.
85. He S, Wang HM, Ogden TE, Ryan SJ. Transplantation of cultured human retinal pigment epithelium into rabbit subretina. Graefes Arch Clin Exp Ophthalmol. 1993;231(12):737–42.
86. Gabrielian K, Oganesian A, Patel SC, Verp MS, Ernest JT. Cellular response in rabbit eyes after human fetal RPE cell transplantation. Graefes Arch Clin Exp Ophthalmol. 1999;237(4):326–35.
87. Lai CC, Gouras P, Doi K, Lu F, Kjeldbye H, Goff SP, Pawliuk R, Leboulch P, Tsang SH. Tracking RPE transplants labeled by retroviral gene transfer with green

fluorescent protein. Invest Ophthalmol Vis Sci. 1999; 40(9):2141–6.
88. Del Priore LV, Tezel TH, Kaplan HJ. Survival of allogeneic porcine retinal pigment epithelial sheets after subretinal transplantation. Invest Ophthalmol Vis Sci. 2004; 45(3):985–92.
89. Dick AD. Influence of microglia on retinal progenitor cell turnover and cell replacement. Eye (Lond) 2009;23(10): 1939–45.
90. Zecher D, van Rooijen N, Rothstein DM, Shlomchik WD, Lakkis FG. An innate response to allogeneic nonself mediated by monocytes. J Immunol. 2009;183(12):7810–6.
91. Bottino R, Fernandez LA, Ricordi C, Lehmann R, Tsan MF, Oliver R, Inverardi L. Transplantation of allogeneic islets of Langerhans in the rat liver: Effects of macrophage depletion on graft survival and microenvironment activation. Diabetes 1998;47(3):316–23.
92. Liu W, Xiao X, Demirci G, Madsen J, Li XC. Innate NK cells and macrophages recognize and reject allogeneic nonself in vivo via different mechanisms. J Immunol. 2012;188(6):2703–11.
93. Slegers TP, van Rooijen N, van Rij G, van der Gaag R. Delayed graft rejection in pre-vascularised corneas after subconjunctival injection of clodronate liposomes. Curr Eye Res. 2000;20(4):322–4.
94. Spangrude GJ, Heimfeld S, Weissman IL. Purification and characterization of mouse hematopoietic stem cells. Science 1988;241(4861):58–62.
95. Lagasse E, Weissman IL. Flow cytometric identification of murine neutrophils and monocytes. J Immunol Methods 1996;197(1–2):139–50.
96. Akimoto H, McDonald TO, Weyhrich JT, Thomas R, Rothnie CL, Allen MD. Antibody to CD18 reduces neutrophil and T lymphocyte infiltration and vascular cell adhesion molecule-1 expression in cardiac rejection. Transplantation 1996;61(11):1610–7.
97. Healy DG, Watson RW, O'Keane C, Egan JJ, McCarthy JF, Hurley J, Fitzpatrick J, Wood AE. Neutrophil transendothelial migration potential predicts rejection severity in human cardiac transplantation. Eur J Cardiothorac Surg. 2006;29(5):760–6.
98. El-Sawy T, Belperio JA, Strieter RM, Remick DG, Fairchild RL. Inhibition of polymorphonuclear leukocyte-mediated graft damage synergizes with short-term costimulatory blockade to prevent cardiac allograft rejection. Circulation 2005;112(3):320–31.
99. Zehr KJ, Herskowitz A, Lee PC, Poston RS, Gillinov AM, Baumgartner WA. Neutrophil adhesion inhibition prolongs survival of cardiac allografts with hyperacute rejection. J Heart Lung Transplant. 1993;12(5):837–44; discussion 844–5.
100. Kaneider NC, Reinisch CM, Dunzendorfer S, Meierhofer C, Djanani A, Wiedermann CJ. Induction of apoptosis and inhibition of migration of inflammatory and vascular wall cells by cerivastatin. Atherosclerosis 2001;158(1): 23–33.
101. Dunzendorfer S, Rothbucher D, Schratzberger P, Reinisch N, Kahler CM, Wiedermann CJ. Mevalonate-dependent inhibition of transendothelial migration and chemotaxis of human peripheral blood neutrophils by pravastatin. Circ Res. 1997;81(6):963–9.
102. Kobashigawa JA, Katznelson S, Laks H, Johnson JA, Yeatman L, Wang XM, Chia D, Terasaki PI, Sabad A, Cogert GA, Trosian K, Hamilton MA, Moriguchi JD, Kawata N, Hage A, Drinkwater DC, Stevenson LW. Effect of pravastatin on outcomes after cardiac transplantation. N Engl J Med. 1995;333(10):621–7.
103. Wenke K, Meiser B, Thiery J, Nagel D, von Scheidt W, Krobot K, Steinbeck G, Seidel D, Reichart B. Simvastatin initiated early after heart transplantation: 8-Year prospective experience. Circulation 2003;107(1):93–7.
104. Wenkel H, Streilein JW. Evidence that retinal pigment epithelium functions as an immune-privileged tissue. Invest Ophthalmol Vis Sci. 2000;41(11):3467–73.
105. Ishida K, Panjwani N, Cao Z, Streilein JW. Participation of pigment epithelium in ocular immune privilege. 3. Epithelia cultured from iris, ciliary body, and retina suppress T-cell activation by partially non-overlapping mechanisms. Ocul Immunol Inflamm. 2003;11(2):91–105.
106. Rosenberg AS, Singer A. Cellular basis of skin allograft rejection: An in vivo model of immune-mediated tissue destruction. Annu Rev Immunol. 1992;10:333–58.
107. Uckermann O, Uhlmann S, Wurm A, Reichenbach A, Wiedemann P, Bringmann A. ADPbetaS evokes microglia activation in the rabbit retina in vivo. Purinergic Signal. 2005;1(4):383–7.
108. Zhang C, Shen JK, Lam TT, Zeng HY, Chiang SK, Yang F, Tso MO. Activation of microglia and chemokines in light-induced retinal degeneration. Mol Vis. 2005;11:887–95.
109. Hume DA, Perry VH, Gordon S. Immunohistochemical localization of a macrophage-specific antigen in developing mouse retina: Phagocytosis of dying neurons and differentiation of microglial cells to form a regular array in the plexiform layers. J Cell Biol. 1983;97(1):253–7.
110. Pinilla I, Cuenca N, Martinez-Navarrete G, Lund RD, Sauve Y. Intraretinal processing following photoreceptor rescue by non-retinal cells. Vision Res. 2009;49(16): 2067–77.
111. Li L, Turner JE. Optimal conditions for long-term photoreceptor cell rescue in RCS rats: The necessity for healthy RPE transplants. Exp Eye Res. 1991;52(6):669–79.
112. Silverman MS, Hughes SE. Photoreceptor rescue in the RCS rat without pigment epithelium transplantation. Curr Eye Res. 1990;9(2):183–91.
113. Kerr EC, Raveney BJ, Copland DA, Dick AD, Nicholson LB. Analysis of retinal cellular infiltrate in experimental autoimmune uveoretinitis reveals multiple regulatory cell populations. J Autoimmun. 2008;31(4):354–61.
114. Daley JM, Thomay AA, Connolly MD, Reichner JS, Albina JE. Use of Ly6G-specific monoclonal antibody to deplete neutrophils in mice. J Leukoc Biol. 2008;83(1):64–70.
115. Kroemer G, Galluzzi L, Vandenabeele P, Abrams J, Alnemri ES, Baehrecke EH, Blagosklonny MV, El-Deiry WS, Golstein P, Green DR, Hengartner M, Knight RA, Kumar S, Lipton SA, Malorni W, Nuñez G, Peter ME, Tschopp J, Yuan J, Piacentini M, Zhivotovsky B, Melino G, Nomenclature Committee on Cell Death 2009. Classification of cell death: Recommendations of the Nomenclature Committee on Cell Death 2009. Cell Death Differ. 2009;16(1):3–11.
116. Galluzzi L, Vitale I, Abrams JM, Alnemri ES, Baehrecke EH, Blagosklonny MV, Dawson TM, Dawson VL, El-Deiry WS, Fulda S, Gottlieb E, Green DR, Hengartner MO, Kepp O, Knight RA, Kumar S, Lipton SA, Lu X, Madeo F, Malorni W, Mehlen P. Molecular definitions of cell death subroutines: Recommendations of the Nomenclature Committee on Cell Death 2012. Cell Death Differ. 2012;19(1):107–20.

117. Liu Y, Levine B. Autosis and autophagic cell death: The dark side of autophagy. Cell Death Differ. 2015;22(3): 367–76.
118. Wei Y, Pattingre S, Sinha S, Bassik M, Levine B. JNK1-mediated phosphorylation of Bcl-2 regulates starvation-induced autophagy. Mol Cell 2008;30(6):678–88.
119. Liu Y, Shoji-Kawata S, Sumpter RM, Jr, Wei Y, Ginet V, Zhang L, Posner B, Tran KA, Green DR, Xavier RJ, Shaw SY, Clarke PG, Puyal J, Levine B. Autosis is a Na+,K+-ATPase-regulated form of cell death triggered by autophagy-inducing peptides, starvation, and hypoxia-ischemia. Proc Natl Acad Sci USA 2013;110 (51):20364–71.
120. Baehrecke EH. Autophagy: Dual roles in life and death? Nat Rev Mol Cell Biol. 2005;6(6):505–10.
121. Galluzzi L, Maiuri MC, Vitale I, Zischka H, Castedo M, Zitvogel L, Kroemer G. Cell death modalities: Classification and pathophysiological implications. Cell Death Differ. 2007;14(7):1237–43.
122. Dai JD, Gilbert LI. Programmed cell death of the prothoracic glands of Manduca sexta during pupal-adult metamorphosis. Insect Biochem Mol Biol. 1997;27(1):69–78.
123. Thorball N, Moe H, Winther-Nielsen H. Progressive involution and physiological death of smooth muscle cells of rat incisal arterioles. Blood Vessels 1985;22(4):157–69.
124. Fink SL, Cookson BT. Apoptosis, pyroptosis, and necrosis: Mechanistic description of dead and dying eukaryotic cells. Infect Immun. 2005;73(4):1907–16.
125. Savill J, Fadok V. Corpse clearance defines the meaning of cell death. Nature 2000;407(6805):784–8.
126. Takeda K, Kaisho T, Akira S. Toll-like receptors. Annu Rev Immunol. 2003;21:335–76.
127. Bianchi ME. DAMPs, PAMPs and alarmins: All we need to know about danger. J Leukoc Biol. 2007;81(1):1–5.
128. Kindzelskii AL, Elner VM, Elner SG, Yang D, Hughes BA, Petty HR. Toll-like receptor 4 (TLR4) of retinal pigment epithelial cells participates in transmembrane signaling in response to photoreceptor outer segments. J Gen Physiol. 2004;124(2):139–49.
129. Elner SG, Petty HR, Elner VM, Yoshida A, Bian ZM, Yang D, Kindezelskii AL. TLR4 mediates human retinal pigment epithelial endotoxin binding and cytokine expression. Trans Am Ophthalmol Soc. 2005;103:126–35; discussion 135–7.
130. Tu Z, Portillo JA, Howell S, Bu H, Subauste CS, Al-Ubaidi MR, Pearlman E, Lin F. Photoreceptor cells constitutively express functional TLR4. J Neuroimmunol. 2011;230(1–2):183–7.
131. Chang JH, McCluskey P, Wakefield D. Expression of toll-like receptor 4 and its associated lipopolysaccharide receptor complex by resident antigen-presenting cells in the human uvea. Invest Ophthalmol Vis Sci. 2004; 45(6):1871–8.
132. Ricklin D, Lambris JD. Complement in immune and inflammatory disorders: Pathophysiological mechanisms. J Immunol. 2013;190(8):3831–8.
133. Prohaszka Z, Singh M, Nagy K, Kiss E, Lakos G, Duba J, Fust G. Heat shock protein 70 is a potent activator of the human complement system. Cell Stress Chaperones 2002;7(1):17–22.
134. Walport MJ. Complement. First of two parts. N Engl J Med. 2001;344(14):1058–66.
135. Markiewski MM, Lambris JD. The role of complement in inflammatory diseases from behind the scenes into the spotlight. Am J Pathol. 2007;171(3):715–27.
136. Nosal R, Drabikova K, Jancinova V, Perecko T, Ambrozova G, Ciz M, Lojek A, Pekarova M, Smidrkal J, Harmatha J. On the molecular pharmacology of resveratrol on oxidative burst inhibition in professional phagocytes. Oxid Med Cell Longev. 2014;2014:706269.
137. Jancinova V, Perecko T, Harmatha J, Nosal R, Drabikova K. Decreased activity and accelerated apoptosis of neutrophils in the presence of natural polyphenols. Interdiscip Toxicol. 2012;5(2):59–64.
138. Wang AL, Yu AC, Lau LT, Lee C, Wu le M, Zhu X, Tso MO. Minocycline inhibits LPS-induced retinal microglia activation. Neurochem Int. 2005;47(1–2):152–8.
139. Krady JK, Basu A, Allen CM, Xu Y, LaNoue KF, Gardner TW, Levison SW. Minocycline reduces proinflammatory cytokine expression, microglial activation, and caspase-3 activation in a rodent model of diabetic retinopathy. Diabetes 2005;54(5):1559–65.
140. Killingsworth MC, Sarks JP, Sarks SH. Macrophages related to Bruch's membrane in age-related macular degeneration. Eye (Lond) 1990;4(Pt 4):613–21.
141. Cherepanoff S, McMenamin P, Gillies MC, Kettle E, Sarks SH. Bruch's membrane and choroidal macrophages in early and advanced age-related macular degeneration. Br J Ophthalmol. 2010;94(7):918–25.
142. van der Schaft TL, Mooy CM, de Bruijn WC, de Jong PT. Early stages of age-related macular degeneration: An immunofluorescence and electron microscopy study. Br J Ophthalmol. 1993;77(10):657–61.